Electronic supplementary information

Metal organic framework derived Nb_2O_5@C nanoparticles grown on reduced graphene oxide for high-energy lithium ion capacitors

Xinyan Jiao, Qingli Hao*, Xifeng Xia, Zongdeng Wu and Wu Lei

Key Laboratory for Soft Chemistry and Functional Materials, Nanjing University of Science and Technology, Ministry of Education, Nanjing 210094, Jiangsu, China. E-mail: qinglihao@njust.edu.cn

21st June 2019
Note added after first publication: This Supplementary Information file replaces that originally published on 12th February 2019, in which the synthesis masses of $NbCl_5$ and 2-methylimidazole should have been expressed in g rather than mg.

.

Experimental section

Materials synthesis: Graphene oxide (GO) was prepared by oxidizing graphite using modified Hummers' method. The M-Nb_2O_5@C/rGO was synthesized as follows: First, 10 mg GO was dispersed in 20 mL methanol and sonicated for 1.5 h. Second, 0.108 g of niobium pentachloride ($NbCl_5$) was added into the GO dispersion followed by stirring for 20 min to form solution A. Third, 0.164 g of 2-methylimidazole was dissolved in 10 mL methanol with stirring for 20 min to form solution B. Then, the solution B was dropwise added into solution A under stirring and the mixed solution was kept undisturbed at ambient temperature for 12 h. The powder product (Nb-MOF/GO) was obtained by centrifugation, washed using methanol and freeze drying. Finally, the Nb-MOF/GO was annealed at 800 ℃ for 2 h under N_2 protection to obtain MOF-derived Nb_2O_5@C/rGO (M-Nb_2O_5 @C/rGO) composites. The M-Nb_2O_5@C composites were prepared via similar procedure without GO.

Material characterizations: The transmission electron microscopy (TEM) was performed on a JEOL JEM-2100F to investigate the morphology of samples. The powder X-ray diffraction (XRD) was obtained on a Bruker D8 Advance diffractometer with Cu Kα radiation to study the crystallographic phases. Fourier transform infrared spectrometer (FT-IR) was tested from a Bruker Vector 22. Raman spectra were recorded on a Renishaw Invia Raman Microscope with a 514.5 nm laser. The X-ray photoelectron spectroscopy (XPS) was carried out using Thermo ESCALAB 250 UK with monochromatic Al Kα radiation (150 W, 1486.6 eV and 500 μm).

Electrochemical measurements: For the electrochemical performances, the 2032 coin-type cells were assembled in argon filled glove box. To obtain the working electrode, active material, conductive carbon black and polyvinylidene fluoride (PVDF) were mixed (8:1:1, weight ratio), and then dissolved into N-methyl-2-pyrrolidone (NMP), coated onto the Cu foil and dried in vacuum oven. The mass loading of the active materials in electrode are ~ 0.8 mg cm^{-1}. A solution of 1 M $LiPF_6$ dissolved in ethylene carbonate (EC)/diethyl carbonate (DEC)/dimethyl carbonate (DMC) (1:1:1 by volume) was used as electrolyte. The cyclic voltammetry (CV) curves and electrochemical impedance spectroscopy (EIS) were conducted on electrochemical workstations (CHI 760C and 1030C, Chenhua, Shanghai China). The galvanostatic charge/discharge measurements under various rates were performed in the potential range of 1-3 V (*vs.* Li^+/Li) on a Land CT2001 (Wuhan China) battery test system.

The Li-ion capacitor (M-Nb_2O_5@C/rGO//AC) were assembled into coin cell with pre-lithiated M-Nb_2O_5@C/rGO as the anode and activated carbon AC as the cathode. The pre-lithiation process of anode was performed using galvanostatic charge/discharge test at current density of 0.2 A g^{-1} with lithium foil as counter electrode. This process was terminated once reaching the 80% of maximum

capacity value. The energy and power densities were also calculated from the galvanostatic charge/discharge curves based on the following equations:

$$E = \int_{t_1}^{t_2} l\,V\,dt = \Delta V \times \frac{l}{m} \times t \quad (1)$$

$$P = \frac{l}{m} = \Delta V \times \frac{l}{m} \quad (2)$$

where E (Wh kg^{-1}) is energy density, P is power density (W kg^{-1}), ΔV (V) is the voltage range, l (A) is the discharge current, t (s) is the discharge time and m (g) is the total mass of anode and cathode active materials.

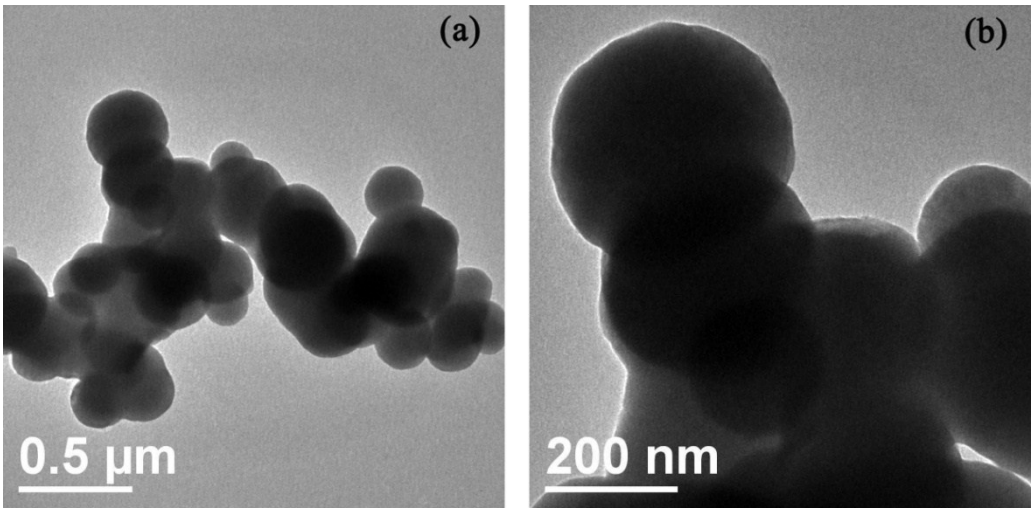

Figure S1 TEM images of M-Nb_2O_5@C

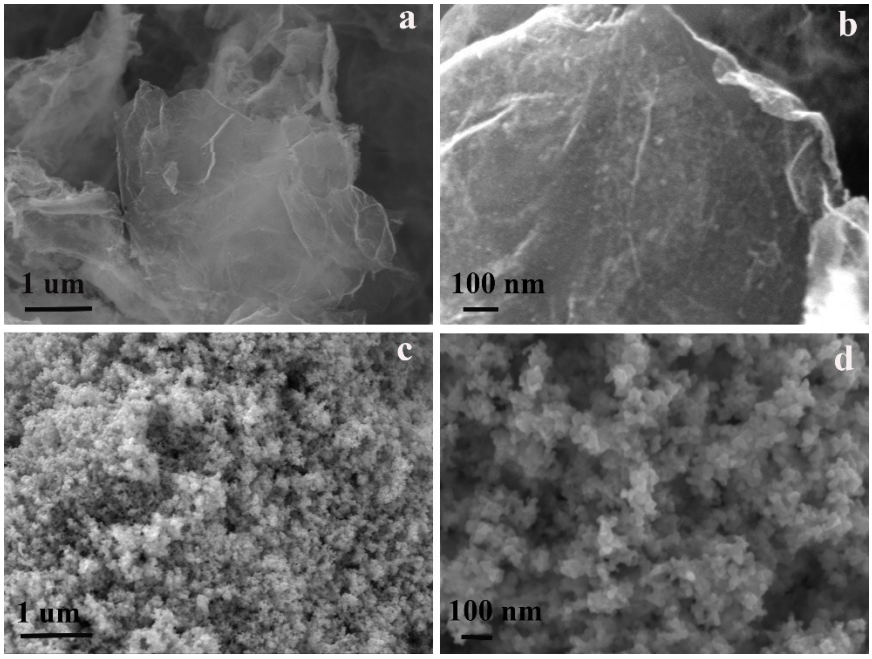

Figure S2 SEM images of M-Nb_2O_5@C/rGO (a, b) and M-Nb_2O_5@C (c, d)

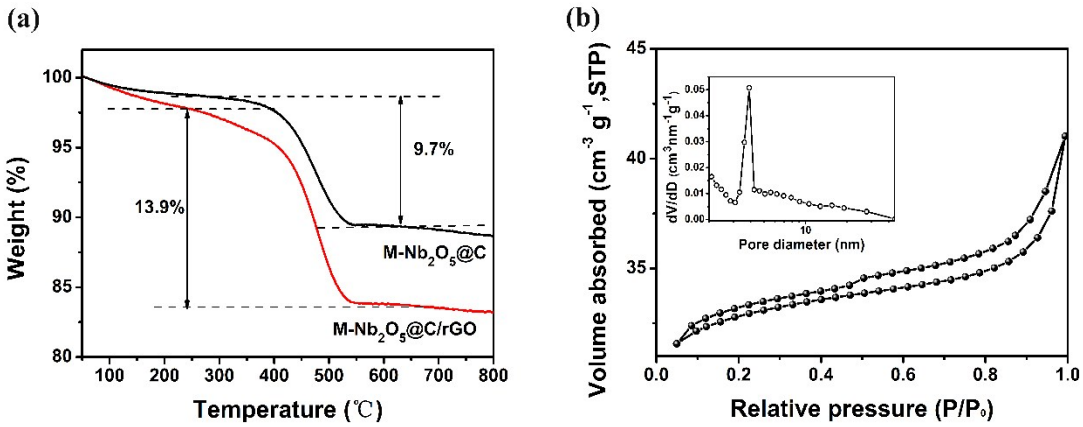

Figure S3 TG analysis of M-Nb_2O_5@C/rGO and M-Nb_2O_5@C (a); Nitrogen adsorption/desorption isotherms and BJH pore size distribution of M-Nb_2O_5@C (b)

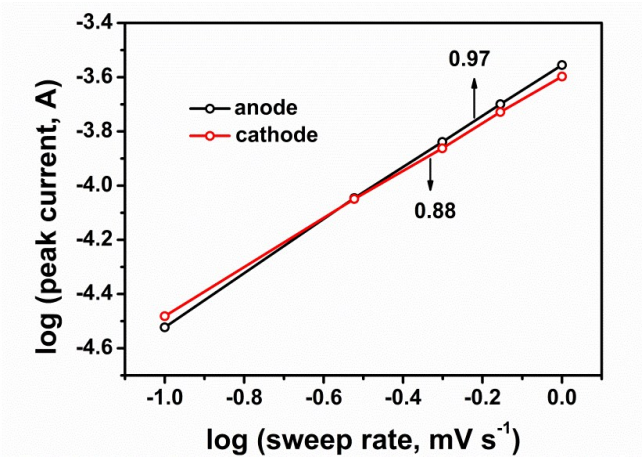

Figure S4 The anode and cathode peak currents at various scan rates of M-Nb_2O_5@C/rGO

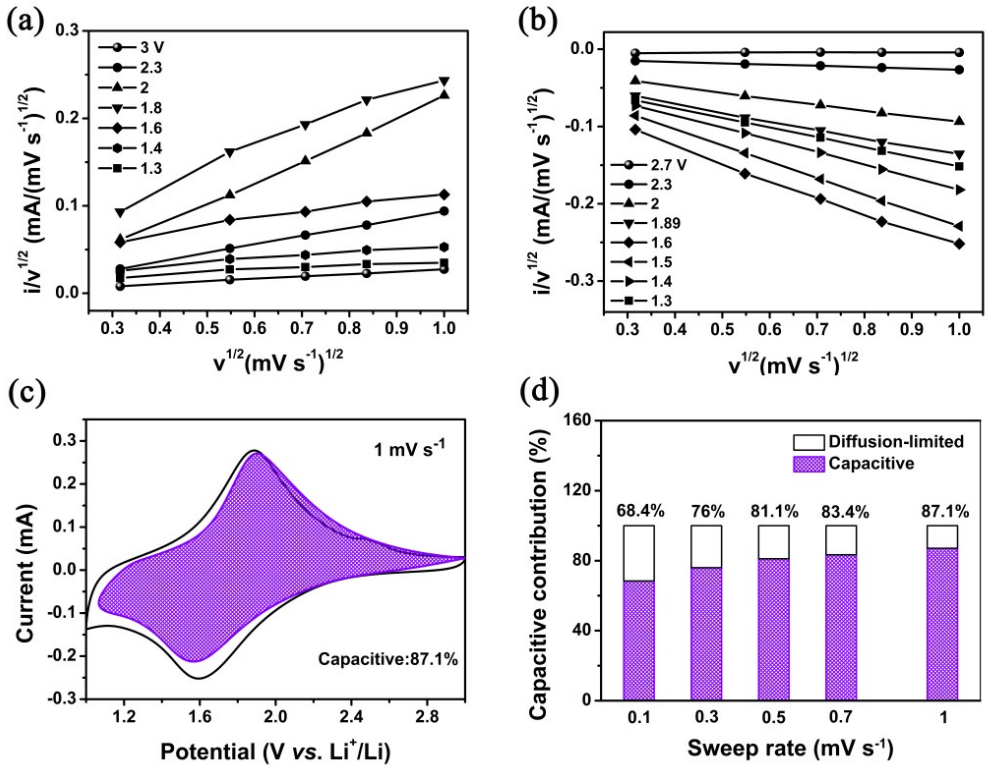

Figure S5 (a) Linear relation of (a) anodic currents and (b) cathodic currents with sweep rates at fixed potential of M-Nb_2O_5@C/rGO; (c) CV curves of M-Nb_2O_5@C/rGO with separation between total current and capacitive current (shaded region) at 1 mV s^{-1}; (d) Capacitive contributions of M-Nb_2O_5@C/rGO at various sweep rates.

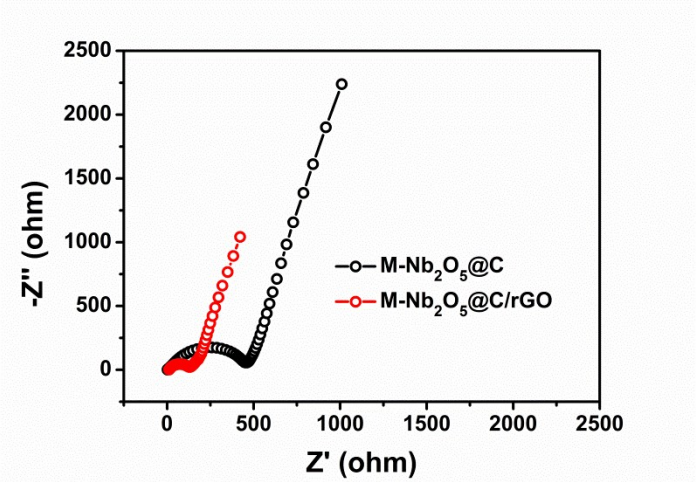

Figure S6 Comparison of Nyquist plots of M-Nb_2O_5@C and M-Nb_2O_5 @C/rGO

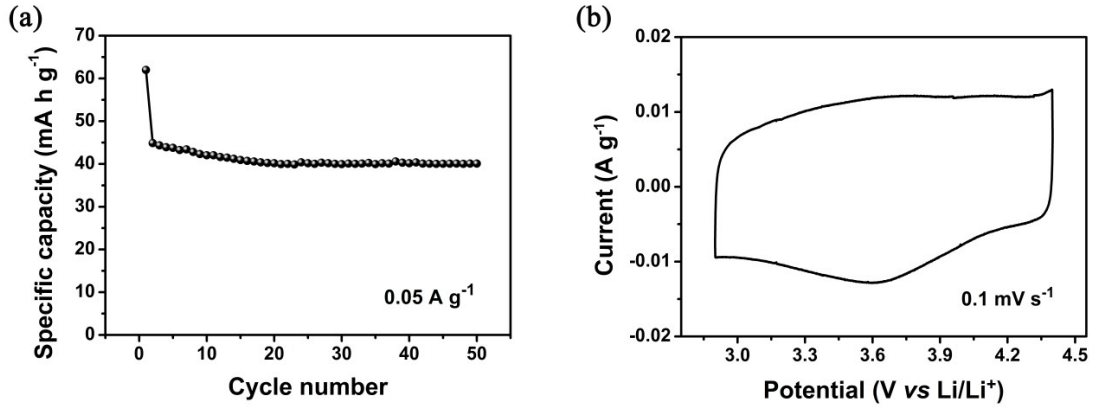

Figure S7 (a) Cycle performance of AC at 0.05 A g^{-1}. (b) CV curve of AC at 0.1 mV s^{-1}.